*Catalysis Letters Vol. 108, Nos. 1–2, April 2006 (© 2006)*
DOI: 10.1007/s10562-006-0023-0


# Methane dehydroaromatization on Mo/HMCM-22 catalysts: effect of $SiO_2/Al_2O_3$ ratio of HMCM-22 zeolite supports

Lin Liu, Ding Ma, Huiying Chen, Heng Zheng, Mojie Cheng, Yide Xu, and Xinhe Bao*

*State Key Laboratory of Catalysis, Dalian Institute of Chemical Physics, Chinese Academy of Sciences, 457 Zhongshan Road, P.O. Box 110, Dalian 116023, P.R. China*

Received 19 November 2005; accepted 19 January 2006

HMCM-22 zeolite with variable $SiO_2/Al_2O_3$ ratios has been successfully synthesized and used as support of molybdenum based catalyst in methane dehydroaromatization. Effect of $SiO_2/Al_2O_3$ ratio on the catalytic performance of Mo/HMCM-22 catalysts was studied, and results show that methane conversion and benzene selectivity increase with the decrease of $SiO_2/Al_2O_3$ ratio, and reach maximum on Mo/HMCM-22 catalyst with $SiO_2/Al_2O_3$ ratio of 25. Further increasing $SiO_2/Al_2O_3$ ratio results a decrease of activity and benzene selectivity. $^{27}Al$ MAS NMR spectroscopy and $NH_3$-TPD techniques were applied to characterize the structure–property relationship of the catalyst. The catalytic performance of Mo/HMCM-22 catalysts in methane dehydroaromatization has been correlated with the Brönsted acidity of HMCM-22 zeolite supports, which may promote not only the methane activation on the Mo carbide sites of Mo/HMCM-22 catalysts, but also further oligomerization of the $CH_x$ surface species towards aromatics products in the reaction.

**KEY WORDS:** methane dehydroaromatization; HMCM-22 zeolite; Mo/HMCM-22 catalyst; $SiO_2/Al_2O_3$ ratio; Brönsted acidity.

## 1. Introduction

Natural gas (mostly methane) is becoming a promising energy source in the 21st century, but now the utilization of the resource is limited by the high cost of transportation [1,2]. Developing efficient utilization processes of abundant natural gas to valuable liquid fuels and petrochemical intermediates has become a field of continuous interest not only from the standpoint of academic research but also from the potential industrial application. In 1993, Xu and his colleagues [3] first reported that methane could be transformed into aromatics of benzene and naphthalene on Mo/HZSM-5 catalyst under nonoxidative conditions at 973 K. Since then, methane dehydroaromatization reaction has received considerable attention during the past 12 years [4–21].

Mo modified HZSM-5 zeolite catalyst is a bi-functional catalyst with a synergic effect between the molybdenum species and the HZSM-5 zeolite, which results in a efficient catalyst for methane dehydroaromatization with a methane conversion of about 10% and benzene selectivity of 50–60% at 973 K [7–9,16–21]. In addition to Mo/HZSM-5, we recently reported that Mo/HMCM-22 catalysts showed better catalytic performance with higher benzene selectivity (ca. 80% in maximum) as well as a better tolerance to carbonaceous deposits, as compared with Mo/HZSM-5 catalyst under the same experimental conditions [22] MCM-22 zeolite possesses two independent multidimensional channel systems, one system is two-dimensional 10-MR sinusoidal inter-layer channel systems, while the other is inter-layer channel systems contains 12-MR super-cages with inner free space of $0.71 \times 0.71 \times 1.82$ nm [23]. The unique catalytic performance of the Mo/HMCM-22 catalyst is probably due to the unusual channel structure of HMCM-22 zeolite [22,24].

It is well accepted that Mo species is the active center for methane activation, whereas acid sites, especially Brönsted acid sites in the channels of zeolites, are responsible for the oligomerization of intermediates and the formation of benzene and other aromatics in methane dehydroaromatization [8,12,14,25–27]. On the other hand, pore size and channel structure of the zeolites are also crucial for the catalyst activity and distribution of products. Methane dehydroaromatization over Mo based catalysts supported on different types of zeolites have been tested, and results show that zeolites with two-dimensional structures and a pore size approximating the dynamic diameter of benzene are good supports for the reaction [28]. Besides the channel structure of zeolites, the Brönsted acid sites of zeolites also play a key role in the reaction as Mo/NaZSM-5 and/or Mo/$Al_2O_3$ catalysts only show no or little activity for the reaction [3,29]. Therefore, the effect of Brönsted acid sites of HZSM-5 zeolite with different $SiO_2/Al_2O_3$ ratios on the catalytic performance of Mo/HZSM-5 catalyst in methane dehydroaromatization has been well investigated. It is reported that the catalytic performance

*To whom correspondence should be addressed.
E-mail: xhbao@dicp.ac.cn

depends substantially on the Brönsted acidity of HZSM-5 zeolite supports [21]. As it is difficult to obtain MCM-22 samples with whole range of $SiO_2/Al_2O_3$ ratios, especially those with $SiO_2/Al_2O_3$ ratio below 30 [23,30], the role of Brönsted acidity of HMCM-22 zeolite in methane dehydroaromatization has not been carefully studied.

In this paper, HMCM-22 zeolites with different $SiO_2/Al_2O_3$ ratios were synthesized through a post synthesis method and used as supports of Mo modified catalysts in methane dehydroaromatization. Effect of $SiO_2/Al_2O_3$ ratio of HMCM-22 supports on the activity and selectivity of Mo/HMCM-22 catalysts was studied and correlated with the acidity of the catalyst.

## 2. Experimental

### 2.1. Catalysts preparation

HMCM-22 zeolite samples with various $SiO_2/Al_2O_3$ ratios were prepared through a post synthesis method according to the previous reports [31,32]. ERB-1 zeolite precursor was firstly synthesized as described in previous reports and then deboronated by calcination at 873 K for 20 h and followed by refluxing in 6.0 M $HNO_3$ for 20 h. This treatment was recycled till all the boron atoms were removed, which resulted in a highly siliceous deboronated framework, which was added under stirring into an aqueous solution of sodium aluminate and hexamethyleneimine (HMI). The resulted mixture had a molar composition of 1.0 deboronated ERB-1 zeolite: $x$ $Al_2O_3$: 1.0 HMI: 30 $H_2O$ ($x = 0.0165 \sim 0.066$). The mixture was transferred into a Teflon-lined stainless-steel autoclave and kept at 423 K for 5 days. The product was filtered, washed, and calcined at 813 K for 10 h. The obtained MCM-22 zeolite was then transformed into HMCM-22 zeolite by an ion exchange with 0.1 M $NH_4NO_3$ solution at 353 K for 24 h and followed by calcined in air at 773 K for 5 h. HMCM-22 zeolites with different $SiO_2/Al_2O_3$ ratios were denoted as HMCM-22($x$), where $x$ was the bulk $SiO_2/Al_2O_3$ ratio in HMCM-22 zeolite. Mo/HMCM-22($x$) catalysts (wt% = 6%) were prepared by impregnating 2.0 g of HMCM-22 zeolite with 4 ml of the aqueous solution containing the desirable amount of ammonium heptamolybdate and then dried at room temperature for 24 h. After dried at 373 K for 8 h and calcined in air at 773 K for 5 h, the catalysts were crushed and sieved to 20–40 mesh granules for catalytic evaluation.

### 2.2. Characterization

X-ray diffraction (XRD) experiments were conducted in air on a Rigaku D/Max 2500 diffractometer using Cu K$\alpha$ radiation ($\lambda = 1.5418$ Å) at room temperature, with instrumental settings of 40 kV and 50 mA. Data were collected in $2\theta$ range from 5° to 50°, with a scanning rate of 5°/min. The amount of Al and Si in the obtained MCM-22 zeolite was determined by X-ray fluorescence (Adamant Spectrometer PW 2400).

All NMR spectra were taken at 9.4 T on a Varian Infinity Plus-400 Spectrometer using 4 mm $ZrO_2$ rotors. $^{27}$Al MAS NMR spectra were recorded at 104.3 MHz using a 0.75 $\mu$s ($\pi/12$) pulse with a 3 s recycle delay and 800 scans. A 1% aqueous $Al(H_2O)_6^{3+}$ solution was used as the reference of chemical shifts, and samples were spun at 8 kHz.

For the $NH_3$–TPD experiment, 0.14 g sample was dried in a flowing He (99.99%, 30 ml/min) at 873 K for 0.5 h prior to adsorption. Pure $NH_3$ was adsorbed until saturation at 323 K, and then the catalyst was flushed with He at the same temperature for 1 h. TPD measurements were conducted from 323 to 900 K with a heating rate of 15 K/min. He (30 ml/min) was used as the carrier gas. The amount of desorbed ammonia was detected with a thermal conductive detector.

### 2.3. Catalytic evaluation

Methane dehydroaromatization reaction was carried out in a continuous flow reactor system equipped with a quartz tube (10 mm id) packed with 1.5 ml of catalyst pellets of 20–40 mesh. A feed gas mixture of 90% $CH_4$ with 10% $N_2$ was purified and then introduced into the reactor at a flow rate of 1500 ml/g h. The reaction was conducted at 973 K under a pressure of 1 atm. The products were analyzed by an on-line gas chromatograph (Varian CP-3800) equipped with a flame ionization detector (FID) for the analysis of $CH_4$, $C_6H_6$, $C_7H_8$, and $C_{10}H_{12}$ and a thermal conductivity detector (TCD) for the analysis of $H_2$, $N_2$,$CH_4$,CO, $C_2H_4$ and $C_2H_6$. $N_2$ (10%) in the feed was used as an internal standard for analyzing all products, including carbonaceous deposition on the basis of converted methane molecules.

## 3. Results and discussion

### 3.1. Characterization

As shown in figure 1, the XRD patterns of obtained HMCM-22 samples agree well with the literature [23,30], proving high crystallinity of the HMCM-22 samples. Through post synthesis method, highly crystalline HMCM-22 zeolite with different $SiO_2/Al_2O_3$ ratios in the range of 19–65 can be obtained.

$^{27}$Al MAS NMR has been used as an efficient probe to determine the coordination and the local structure, as well as the geometry, of specific aluminum species in zeolites. The quantity and location of Al atoms in HMCM-22 zeolite with different $SiO_2/Al_2O_3$ ratios are characterized by $^{27}$Al MAS NMR spectroscopy. Besides a peak centered at 0 ppm characterized corresponding to the octahedral nonframework Al species, two peaks

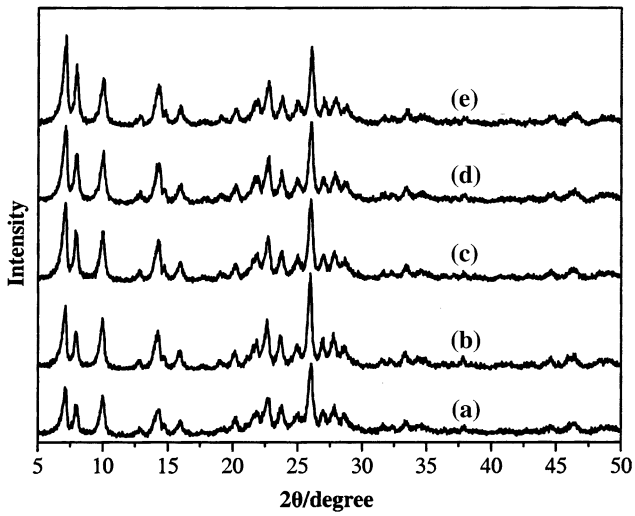


Figure 1. XRD patterns of HMCM-22 zeolite with different $SiO_2/Al_2O_3$ ratios: (a) 19; (b) 25; (c) 35; (d) 43; (e) 65.

centered at ~50 and ~55 ppm corresponding to the different tetrahedral framework Al species can be observed on all samples (figure 2). In the case of HMCM-22 zeolite with $SiO_2/Al_2O_3$ ratio of 19, an additional broad resonance at about ca. 30 ppm can be clearly resolved. It can be attributed to 5-coordinated nonframework Al species [33]. The relative resonance intensities of peak at ~ 50 and ~55 ppm are well consistent with the Al content in HMCM-22 zeolite. As shown in figure 2, the peaks corresponding to the framework Al increase gradually in intensity with the decrease of $SiO_2/Al_2O_3$ ratios from 65 to 25. However, the intensity of 50 and 55 ppm peaks corresponding to the framework Al species decreased when the $SiO_2/Al_2O_3$ ratio further decreased from 25 to 19. Coupling with the appearance of 30 ppm peak corresponding to the 5-coordinated nonframework Al species in the case of HMCM-22(19), it is clear that $SiO_2/Al_2O_3$ ratio of 25 is the maximum content that Al can incorporate into the MCM-22 zeolite framework, while additional Al will exist as nonframework Al species.

$NH_3$-TPD can give out the information not only about the amount of the acid sites but also about the acid strength distribution. The acidity of the HMCM-22 zeolites with different $SiO_2/Al_2O_3$ ratios was investigated by $NH_3$–TPD. As shown in figure 3, three desorption peaks centered at about 550, 720, and 840 K are observed for all samples, which is comparable to those reported in literature for HMCM-22 zeolite [32]. The first peak at 550 K in figure 3 can be assigned to the adsorption of $NH_3$ over weak acid sties probably associated with nonframework octahedral Al species. Its intensity decreases gradually with the increase of $SiO_2/Al_2O_3$ ratios, which is in accordance with the decreasing intensity of the resonance peak at 0 ppm (octahedral Al) in the $^{27}Al$ MAS NMR spectra (figure 2). The high temperature desorption peak at about 720 K is attributed to the adsorbed $NH_3$ molecules over the Brönsted acid sites, and the intensity of which increases remarkably with the decrease of $SiO_2/Al_2O_3$ ratios from 65 to 25, while a further increase of $SiO_2/Al_2O_3$ ratio to 19 leads to a decrease in intensity of desorption peak at about 720 K, although the total Al content of HMCM-22(19) is much higher. This result suggests that only framework tetrahedral Al species contribute to the Brönsted acid sites. This is in good agreement with the $^{27}Al$ MAS NMR experiments that HMCM-22(19) has a lower intensity of 50 and 55 ppm peaks compared with HMCM-22(25), suggesting that only framework Al species contribute to the Brönsted acid sites. The desorption peak at 873 K might correspond to strong Lewis acid sites, and HMCM-22(25) shows the highest

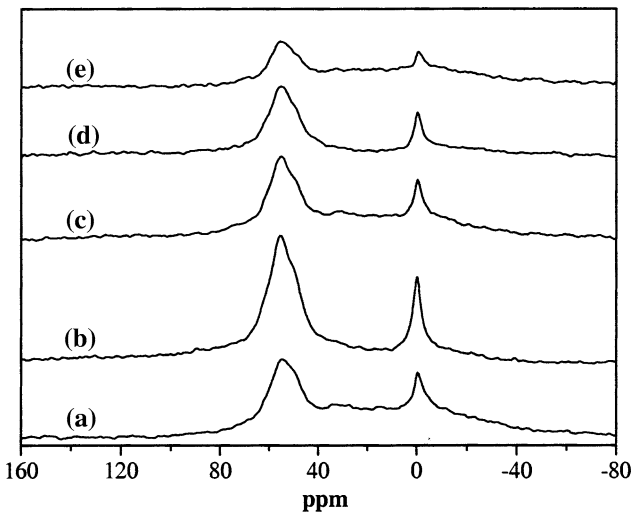


Figure 2. $^{27}Al$ MAS NMR spectra of HMCM-22 zeolite with different $SiO_2/Al_2O_3$ ratios: (a) 19; (b) 25; (c) 35; (d) 43; (e) 65.

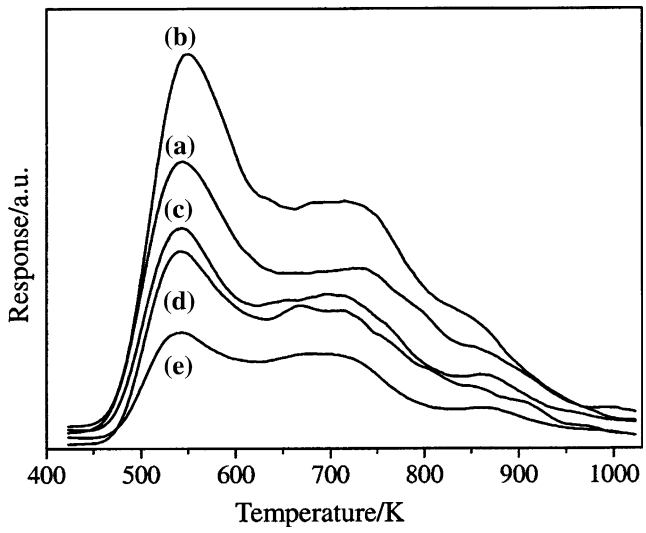


Figure 3. $NH_3$–TPD profiles of HMCM-22 zeolite with different $SiO_2/Al_2O_3$ ratios: (a) 19; (b) 25; (c) 35; (d) 43; (e) 65.

strong Lewis acid sites among the samples with $SiO_2/Al_2O_3$ ratio ranging from 65 to 19.

From above discussion, we can conclude that Brönsted acid sites in HMCM-22 zeolite increase gradually with the decreasing $SiO_2/Al_2O_3$ ratio from 65 to 25, and show a maximum value on HMCM-22(25); further decrease of $SiO_2/Al_2O_3$ ratio in HMCM-22 zeolite results a decrease in the amount of Brönsted acid sites.

### 3.2. *Effects of $SiO_2/Al_2O_3$ ratio on the activity, selectivity, and stability of Mo/HMCM-22 catalysts*

Figure 4 shows methane conversion of Mo/HMCM-22 catalysts with time on-stream at 973 K. The initial methane conversion of Mo/HMCM-22 catalyst with 1 h time on-stream increases with the decrease of $SiO_2/Al_2O_3$ ratios (from 65 to 25), further decrease of the $SiO_2/Al_2O_3$ ratio to 19 results in a decrease in initial methane conversion. For all the samples, the methane conversion usually decreases rapidly in the initial period of the reaction and is relatively stable at the later stage of the reaction. The decrease of methane conversion may be attributed to coke formation on the Mo/HMCM-22 catalysts. The coke deposits may mask the Brönsted acid sites and will eventually lead to the blockage of the channels/pores of the zeolite, thus making the active sites inaccessible for the reactant and other reaction intermediates. This result suggests that the deposited carbon leads to the gradual deactivation of the catalyst and thus the catalyst becomes less reactive with time on-stream. Among five Mo/HMCM-22 catalysts with different $SiO_2/Al_2O_3$ ratios, Mo/HMCM-22(25) gives a much stable catalytic performance and the activity of the Mo/HMCM-22(25) decreases only about 21% after 10 h. For Mo/HMCM-22 catalysts with lower $SiO_2/Al_2O_3$ ratio of 19, the methane conversion decreased from 12.4% to 4.2% after 10 h. The activity decreased much rapidly for the Mo/HMCM-22 catalysts with higher $SiO_2/Al_2O_3$ ratios. For example, for the Mo/HMCM22(35) catalyst, the methane conversion decreased from 12.2% to 6.1% after 10 h. The aromatics yields of Mo/HMCM-22 catalysts with time on-stream are shown in figure 5. The yield of aromatics products of Mo/HMCM-22(25) catalyst increased greatly and reaches the maximum (7.1%) after 3 h reaction and stays almost the same (around 7%) with further time on stream. During the initial induction period, the Mo species of the Mo/HMCM-22 catalysts will certainly be reduced and transformed into the active Mo species ($Mo_2C$, or into $Mo_2O_xC_y$), which are responsible for the initial formation of hydrogen and benzene [7–12]. Compared with Mo/HMCM-22(25) catalyst, the aromatics yield of Mo/HMCM-22 catalysts with higher $SiO_2/Al_2O_3$ ratios give a much lower yield of aromatics products. For example, the maximum yield of aromatics products is 4.1% on Mo/HMCM-22(35) catalyst. For Mo/HMCM-22 with a lower $SiO_2/Al_2O_3$ ratio of 19, the maximum yield of aromatics products is only 3.6%.

Effect of $SiO_2/Al_2O_3$ ratio on the activity and selectivity of Mo/HMCM-22 catalysts in methane dehydroaromatization (after 3 h reaction) has been studied and the results are shown in table 1. Figures 6 and 7 more directly show the methane conversion, yield of aromatics, and distribution of various products on Mo/HMCM-22 catalysts with different $SiO_2/Al_2O_3$ ratios after at 973 K for 3 h. From figure 6, it is clear that methane dehydrogenation on Mo/HMCM-22 catalysts depends substantially on the $SiO_2/Al_2O_3$ ratio of HMCM-22 zeolite supports. Methane conversion increases with decrease of $SiO_2/Al_2O_3$ ratio, and reaches maximum (12.5%) on Mo/HMCM-22(25); further decrease of the $SiO_2/Al_2O_3$ ratio (Mo/HMCM-22(19)) results a decrease (8.0%). Effect of $SiO_2/Al_2O_3$ ratio on the distribution of products on Mo/HMCM-22 catalysts

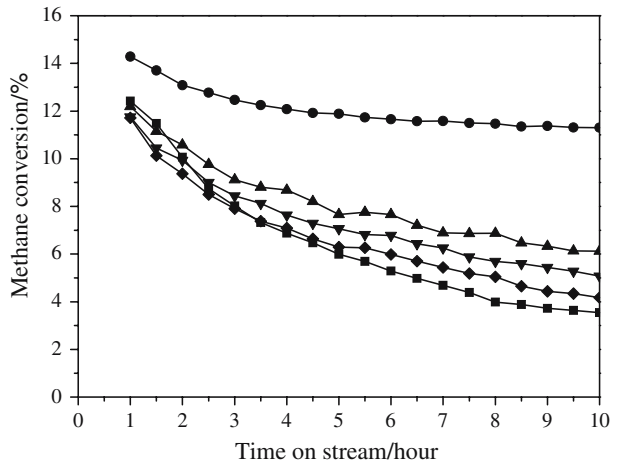


Figure 4. Methane conversion of Mo/HMCM-22 catalysts with different $SiO_2/Al_2O_3$ ratios: (■) 19; (●) 25; (▲) 35; (▼) 43; (◆) 65. Reaction conditions: T = 973 K, 1 atm, GHSV = 1.500 $h^{-1}$.

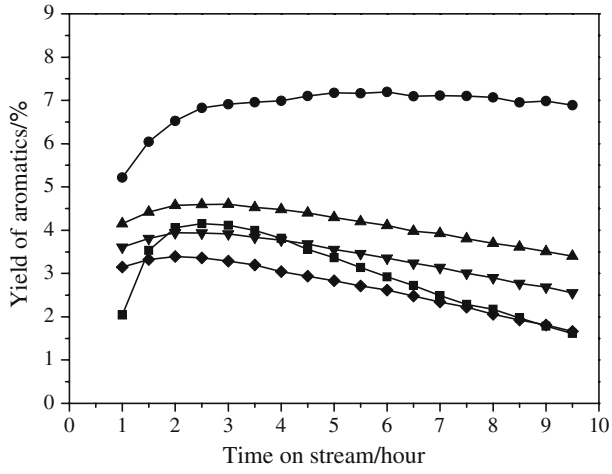


Figure 5. Yield of aromatics products of Mo/HMCM-22 catalysts with different $SiO_2/Al_2O_3$ ratios: (■) 19; (●) 25; (▲) 35; (▼) 43; (◆) 65. Reaction conditions: T = 973 K, 1 atm, GHSV = 1500 $h^{-1}$.

Table 1
Catalytic performance of Mo/HMCM-22 catalysts with different $SiO_2/Al_2O_3$ ratios

| Catalyst | Methane conversion (%) | Selectivity (%) | | | | | Yields of aromatics (%) |
|---|---|---|---|---|---|---|---|
| | | Benzene | Toluene | Naphthalene | $C_2^=$ | Coke | |
| Mo/HMCM-22(19) | 8.0 | 44.7 | 1.8 | 4.8 | 3.8 | 44.8 | 4.1 |
| Mo/HMCM-22(25) | 12.5 | 48.0 | 1.9 | 5.4 | 2.2 | 42.5 | 6.9 |
| Mo/HMCM-22(35) | 9.1 | 43.1 | 1.8 | 5.5 | 3.2 | 46.4 | 4.6 |
| Mo/HMCM-22(43) | 8.4 | 39.0 | 1.7 | 5.9 | 3.6 | 49.8 | 3.9 |
| Mo/HMCM-22(65) | 7.9 | 35.7 | 1.6 | 5.2 | 3.8 | 53.8 | 3.4 |

*Note*: Time on-stream = 3 h; Reaction temperature: 973 K; Reaction pressure: 1 atm; GHSV = 1500 $h^{-1}$.

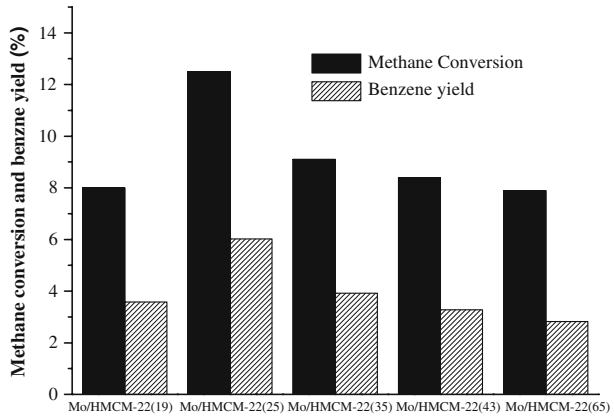


Figure 6. Methane conversion, and benzene yield of Mo/HMCM-22 catalysts after 3h time-on-stream of methane dehydroaromatization reaction (973 K, 1 atm, GHSV = 1500 $h^{-1}$).

was also examined after running for 3 h. As shown in figure 7, $SiO_2/Al_2O_3$ ratio of HMCM-22 zeolite supports is an important factor for methane dehydroaromatization over Mo/HMCM-22 catalysts. Follow the same trend as the activity, benzene selectivity also shows a maximum (45.6%) on the Mo/HMCM-22(25) catalyst. Instead, coke selectivity decreases with decreasing $SiO_2/Al_2O_3$ ratio, and reaches its minimum value (42.5%) on Mo/HMCM-22(25); further decrease of the $SiO_2/Al_2O_3$ ratio results an increase (44.8%) on Mo/HMCM-22(19). Combined with the above results, it can be concluded that the improvement in catalytic performance can be attributed not only to the improvement in methane conversion and benzene selectivity, but also to the decrease in the coke selectivity.

What leads to the different catalytic performance over Mo/HMCM-22 catalysts with different $SiO_2/Al_2O_3$ ratios? It is well known that the channel structure and acidity of zeolite supports are crucial to get a good catalytic performance for methane dehydroaromatization over molybdenum modified zeolite catalyst. Methane activation and benzene formation need channels with diameter of 0.6 nm to accommodate $MoC_x$, species [12]. As all the HMCM-22 zeolite samples share the same structure, the change of activity and benzene selectivity of Mo/HMCM-22 catalysts is inevitably related to the change of acidity of the HMCM-22 zeolite. The variations of Brönsted acidity (deduced from $NH_3$–TPD) of the HMCM-22 zeolite supports and methane conversion, selectivities of benzene and coke of Mo/HMCM-22 catalysts with 3 h reaction are illustrated against the function of $SiO_2/Al_2O_3$ ratios of the HMCM-22 zeolite supports (figure 8). The Brönsted

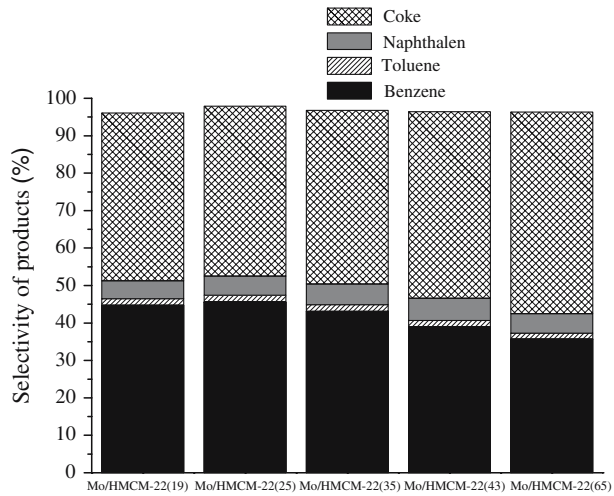


Figure 7. Products distribution of Mo/HMCM-22 catalysts after 3h time-on-stream of methane dehydroaromatization reaction (973 K, 1 atm, GHSV = 1500 $h^{-1}$).

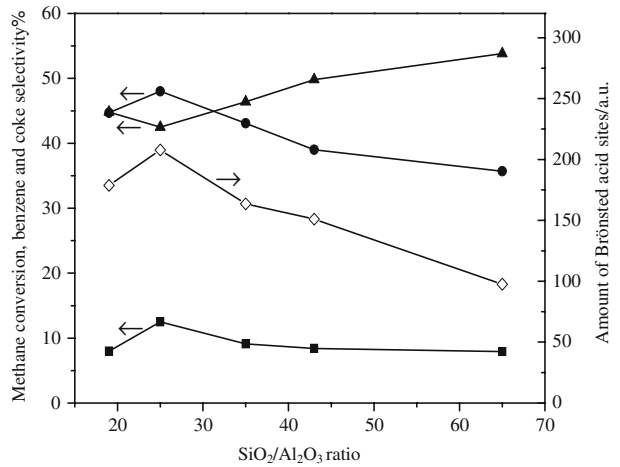


Figure 8. Dependencies of methane conversion (■), selectivity of benzene (●) and coke (▲) of Mo/HMCM-22 catalysts and those of the Brönsted acidity of HMCM-22 zeolite (◇) upon the $SiO_2/Al_2O_3$ ratios (deduced by $NH_3$-TPD).

acidity of HMCM-22 zeolite shows the maximum on HMCM-22(25), which is identical to that of methane conversion and benzene selectivity; at the same time, coke selectivity shows minimum on the Mo/HMCM-22(25) catalyst. Based on the close correlation between the Brönsted acidity of Mo/HMCM-22 catalysts and catalytic performance, it is reasonable to suggest that Brönsted acid sites of HMCM-22 zeolite supports, are benefit not only for the activation of methane on $Mo_2C$ and/or $MoC_xO_y$, but also for the subsequently aromatization of the $CH_x$ intermediates, especially for the formation of benzene on the Mo/HMCM-22 catalysts.

## 4. Conclusions

Coupling the characterization results with the reaction data, correlation between the catalytic performance of Mo/HMCM-22 catalysts in methane dehydroaromatization and Brönsted acidity of HMCM-22 supports are explored systematically. HMCM-22 zeolite with more Brönsted acid sites present higher catalytic activity and benzene selectivity, and reach the maximum value on the Mo/HMCM-22 catalyst with a $SiO_2/Al_2O_3$ ratio of 25, which has maximum Brönsted acid sites. Thus in methane dehydroaromatization reaction, the Brönsted acidity of HMCM-22 zeolite supports may promote not only the methane activation on the Mo carbide sites of Mo/HMCM-22 catalysts, but also a further oligomerization of the dissociative $CH_x$ surface species towards benzene.

## Acknowledgments

The authors gratefully acknowledge the financial support of the National Natural Science Foundation of China (No. 20173062) and the Ministry of Science and Technology of China.

## References

[1] R.H. Crabtree, Chem. Rev. 95 (1995) 987.
[2] M.G. Axelrod, A.M. Gaffney, R. Pitchai and J.A. Sofranko, *in*: *Natural Gas Conversion II*, eds. H.E. Curry-Hyde and R.F. Howe (Elsevier, New York, 1994) p. 93.
[3] L.S. Wang, L.X. Tao, M.S. Xie, G. Xu, J. Huang and Y.D. Xu, Catal. Lett. 21 (1993) 35.
[4] F. Solymosi, A. Erdhelyi and A. Szöke, Catal. Lett. 32 (1995) 43.
[5] D. Wang, J.H. Lunsford and M.P. Rosynek, Topics Catal. 3 (1996) 289.
[6] Y.D. Xu, W. Liu, S.T. Wong, L.S. Wang and X.X. Guo, Catal. Lett. 40 (1996) 207.
[7] F. Solymosi, A. Szöke and J. Cserényi, Catal. Lett. 39 (1996) 157.
[8] F. Solymosi, J. Cserényi, A. Szöke, T. Bansagi and A. Dszko, J. Catal. 165 (1997) 150.
[9] D. Wang, J.H. Lunsford and M.P. Rosynek, J. Catal. 169 (1997) 347.
[10] B.M. Weckhuysen, D. Wang, M.P. Rosynek and J.H. Lunsford, J. Catal. 175 (1998) 338.
[11] Y. Lu, Z.S. Xu, Z.J. Tian, T. Zhang and L.W. Lin, Catal. Lett. 62 (1999) 215.
[12] R.W. Borry III, Y.H. Kim, A. Huffsmith, J.A. Reimer and E. Iglesia, J. Phys. Chem. B 103 (1999) 5787.
[13] Y.D Xu, X.H Bao and L.W. Lin, J. Catal. 216 (2003) 386.
[14] W. Li, G.D. Meitzner, R.W. Borry III and E. Iglesia, J. Catal. 191 (2000) 373.
[15] L.S. Wang, R. Ohnishi and M. Ichikawa, Catal. Lett. 62 (1999) 29.
[16] Vu. Ha, T.T. Tiep, V. Le, P. Meriaudeau and C. Naccache, J. Mol. Catal. A 181 (2002) 283.
[17] Y. Kim, R.W. Borry III and E. Iglesia, Micropor. Mesopor. Mater. 35–36 (2000) 495.
[18] D. Ma, Y.Y. Shu, W.P. Zhang, X.W. Han, Y.D. Xu and X.H. Bao, Angew. Chem., Int. Ed. Engl. 39 (2000) 2928; D. Ma, Y.Y. Shu,M.J. Cheng, Y.D. Xu, X.H. Bao, J. Catal. 194 (2000) 105.
[19] A. Sarioğian, A. Erdem-Senatalar, Ö.T. Savasçi, Y. Ben. Taârit, J. Catal. 228 (2004) 114; A. Sarioğian, A. Erdem-Senatalar, Ö.T. Savasçi, Y. Ben. Taârit, J. Catal. 226 (2004) 210.
[20] P.L. Tan, Y.L. Leung, S.Y. Lai, C.T. Au, Catal. Lett. 78 (2002) 251; P.L. Tan, Y.L. Leung, S.Y. Lai, C.T. Au, Appl. Catal. A 253 (2003) 305.
[21] S.T. Liu, L.S. Wang, R. Ohnishi and M. Ichikawa, J. Catal. 181 (1999) 175.
[22] Y.Y. Shu, D. Ma, L.Y. Xu, Y.D. Xu and X.H. Bao, Catal. Lett. 70 (2000) 67.
[23] A. Corma, C. Corell and J. Perez-Pariente, Zeolites 15 (1995) 2.
[24] D. Ma, Q.J. Zhu, Z.L. Wu, D.H. Zhou, Y.Y. Shu, Q. Xin, Y.D. Xu and X.H. Bao, Phys. Chem. Chem. Phys. 7 (2005) 3102.
[25] F. Solymosi, A. Szöke and J. Cserényi, Appl. Catal. A 142 (1996) 361.
[26] D. Wang, J.H. Lunsford and M.P. Rosynek, Topics Catal. 3 (1996) 289.
[27] S.T. Liu, L.S. Wang, Q. Dong, R. Ohnishi and M. Ichikawa, Stud. Surf. Sci. Catal. 119 (1998) 241.
[28] C.L. Zhang, S. Li, Y. Yuan, W.X. Zhang, T.B. Wu and L.W. Lin, Catal. Lett. 56 (1998) 207.
[29] Y.D. Xu, S.T. Liu, L.S. Wang, M.S. Xie and X.X. Guo, Catal. Lett. 30 (1995) 135.
[30] M.J. Cheng, D.L. Tan, X.M. Liu, X.H. Han, X.H. Bao and L.W. Lin, Micropor. Mesopor. Mater. 42 (2001) 307.
[31] P. Wu and T. Tatsumi, Chem. Commun. 10 (2002) 1026.
[32] S. Unverricht, M. Hunger, S. Ernst, H.G. Karge and J. Weitkamp, Stud. Surf. Sci. Catal. 84 (1994) 37.
[33] D. Ma, F. Deng, R. Fu, X. Han and X. Bao, J. Phys. Chem. B 105 (2001) 1770.